Mariusz Stępień, Zygmunt Mikno

The Reduction of Welding Current Asymmetry in Multispot Welding Machines by Differentiating the Cross-Section of Welding Machine Arms

Abstract: The article discusses the analysis of the propagation of current in resistance multispot welding machines and the adjustment of the cross-section of the welding machine arms aimed to compensate the asymmetry of welding current in individual welds. The analysis involved the effect of the length of multispot welding machines where the span of the arms (distance between welds) amounted up to 2 m, the arms were characterised by various cross-sections and the structural material was characterised by various resistivity (resulting from changes in temperature). The analysis was performed in relation to welding machines using a nominal welding current of 5 kA. The tests made it possible to determine the effect of changes in the value of current on the cross-section of the weld nugget.

Keywords: resistance welding, multispot welding machines, welding current, resistance of welding machine arms

DOI: *10.17729/ebis.2020.4/3*

Introduction

Because of the efficiency of welding power sources in relation to welds requiring low or medium values of elementary welding current, multispot resistance welding is becoming increasingly popular in many industrial applications. The simultaneous joining of many spots through welding is usually required because of specific technological reasons, e.g. to maintain the shape of an element subjected to processing or to prevent its deformation. The multispot resistance welding method is used to make grids, latticework or other large-sized structural elements. The specific nature of the above-named welding process requires the simultaneous supply of current to welds located at various distances from the welding power source. The resistivity of the current circuit, usually composed of arms characterised by the same cross-section, is responsible for the reduction of welding current. Because of the fact that the reduction of welding current varies depending on specific welds, it is not possible to compensate the current by increasing the output voltage at the rectifier. It is, therefore, necessary to apply other procedures enabling the obtainment of expulsion risk-free welds characterised by appropriate strength and, consequently, diameter. The article discusses the possibility of compensating the welding machine arms

Mariusz Stępień – Silesian University of Technology, Faculty of Electrical Engineering;
Zygmunt Mikno – Łukasiewicz Research Network – Instytut Spawalnictwa

supplying current to welds located at various distances from the welding power source. The above-named desired result can be obtained by differentiating the cross-sections of the welding machine arms. The research work discussed in the article also involved the performance of detailed analysis of to what extent changes of the lengths of multispot welding machine arms could reduce welding current or, in other words, how the length of the arms could affect the diameter of the weld nugget. The analysis was based on simplified analytical calculations and FEM modelling.

Multispot resistance welding technology

Multispot resistance welding machines have constituted a certain niche on the welding equipment market, yet recently they have been enjoying growing popularity in various industrial sectors. Multispot welding is usually used to join bars and sections characterised by relatively small dimensions (requiring welding current of several kiloamperes) and made of low-alloy steels. Elements made using multispot welding include fence grids and panels, construction mats, ceiling reinforcement elements or open-work warehouse shelf structures [1]. The above-named components, usually characterised by significant length, are not affected by significant stresses and deformations. The multispot resistance welding process is characterised by significantly higher efficiency than that of classical spot (single-spot) welding. Multispot welding machines enable the making of tens of welds at the same time. Usually, the powering of welding machines having many welding spots is divided into sections so that one source (e.g. one welding transformer) powers between several and twenty spots [2]. The multispot welding processes are performed using both AC (50Hz) and DC (inverter) welding machines [3].

The above-presented multispot welding technology and the characteristics of welded elements indicate that, as regards the quality of the technological process (homogeneity of welds) and the efficiency of the welding process (energy-saving), important multispot welding process-related issues include the manner of supplying current to each weld and, consequently, the design of welding machine arms.

Characteristics of input data subjected to analysis

The analysis of the propagation of current in multispot welding machines was performed in relation to a specific set of input data, defining the range of analysis and necessary reductions/simplifications. The range of data for analysis made it possible to define the parameters of the welding machine and those of the welding process, whereas reduction assumptions enabled the significant reduction of required computational efficiency at the expense of only a slight divergence between the detailed and the simplified data. The size of the divergence was identified by comparing the analytical model with the FEM-based numerical model.

The comparative analysis was performed assuming that the nominal value of current required to make a proper weld amounted to 5 kA, whereas the averaged value of voltage drop (during the process) on the element subjected to welding amounted to 2 V. The tests also assumed the nominal (basic) design of the welding machine arms made of copper and having a defined length and cross-section and, consequently, resistance. The foregoing was used to determine nominal supply voltage (output voltage at the rectifier), which was constant in relation to the entire comparative analysis and made it possible to identify the variability of welding current in the function of the shape of the supply circuit (welding machine arms). The adopted primary arms design data included the total length of an arm (distance from the point of supply to the spot subjected to welding) amounting to 1000 mm and the cross-section of the arms (along the entire length) amounting to

1000 mm². In addition, it was assumed that the total resistance of both arms was by 20% higher than that resulting from the above-named dimensions, constituting the resistance of mechanical joints (contacts) present in the supply circuit. In relation to the welding machine dimensions, the comparative analysis was performed within the span of the arms restricted within the range of 400 mm to 2400 mm and the cross-section of the arms restricted within the range of 400 mm² to 2000 mm². The comparison also involved four different values of material resistivity corresponding to various operating temperatures of the arms i.e. 59 MS/m (conductivity of cold arms – 20°C), 55 MS/m (primary conductivity in relation to a temperature of 38°C), 51 MS/m (conductivity in relation to an elevated temperature of 60°C) and 46 MS/m (conductivity in relation to a limit temperature of 95°C).

There are two groups of reducing assumptions, i.e. assumptions related to simplified analytical calculations and simplifications related to FEM-based numerical modelling. In the first case it was assumed that the drop of voltage was proportional to the length of the arm and that current density was entirely uniform along the entire length of the arm. The voltage drops related to the individual sections of the arms were added and increased by the voltage drops on the joints. The base voltage obtained in relation to the analysis amounted to 2.2 V. In the numerical analysis related to the 3D FEM model, the adopted resistivity of the material was constant. The distribution of current density was identified using the computer. In addition, the resistivity of the joints was modelled as a thin layer of material characterised by appropriately higher resistivity. In relation to the above-presented model, the nominal voltage amounted to 2.518 V and was slightly higher than the voltage determined in the simplified model. Importantly, the percentage changes in the value of current resulting from the changes in the length and the cross-section of the arms were the same in relation to both models, which confirmed their correctness within the range of the previously adopted reducing assumptions.

Numerical model of the multispot welding machine

Calculations subjected to analysis were performed on the basis of numerical models involving the simplified geometry of welding machine arms. The design of the arms subjected to analysis was presented schematically in Figure 1 and included the fragment of the welding machine circuit from the output terminals of the rectifier treated as the welding power source. The arms of the welding machine consisted of four cuboidal sections having the constant cross-section. The above-named elements were connected by mechanical joints characterised by higher resistance. In the comparative analysis, the longest arm section visible in Figure 1 was treated as an element of variable length (the remaining elements of the arm always had the same length). The calculation method based on the aforesaid model was dependent on the type of analysis.

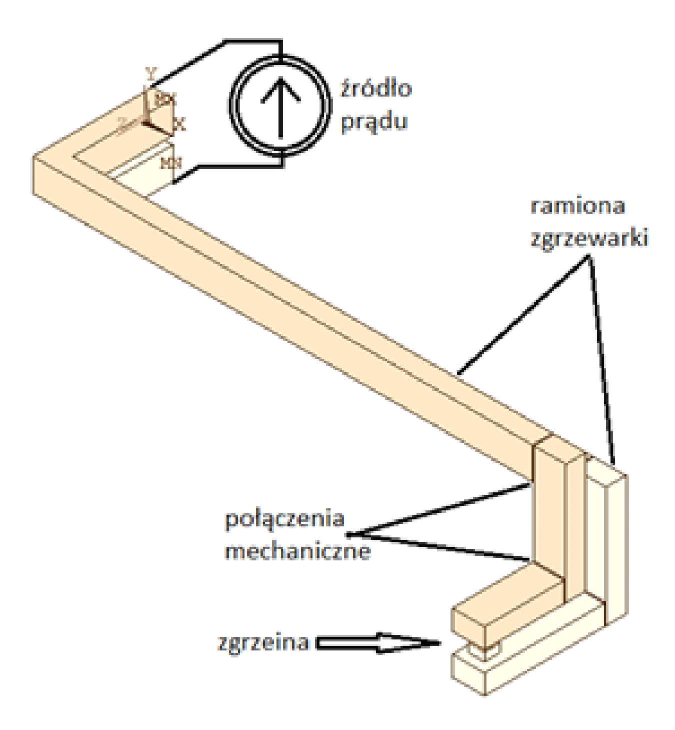

Fig. 1. Structure of the multispot welding machine arm (current supplied to one spot) with the power supply and the area where the weld was formed

In relation to the simplified analytical model, the resistance of the circuit of the arms was determined as the sum of the resistances of the component sections resulting from their geometry. The formula used to identify the resistance of the circuit of the arms was the following (1):

$$R_{arm} = \frac{\sum l_i}{\gamma_{Cu} s_{arm}}$$

where R_{arm} – resistance of the arms without the resistance of the mechanical joints, γ_{Cu} – conductivity of the material at given temperature, s_{arm} – cross-section of the arm (constant along the entire length), l_i – length of the ith section of the arm. In the above-named model, welding current I_{zg} was determined using the following dependence (2):

$$I_{zg} = \frac{U_z}{R_{zg} + R_{arm} + 20\% \cdot R_{arm}}$$

where U_z = 2.2 V – supply voltage. The resistance of the arms increased by 20% reflected the resistance of the mechanical joints. Power supplied to weld P_{zg} was expressed by the following dependence (3):

$$P_{zg} = R_{zg} \cdot I_{zg}^2$$

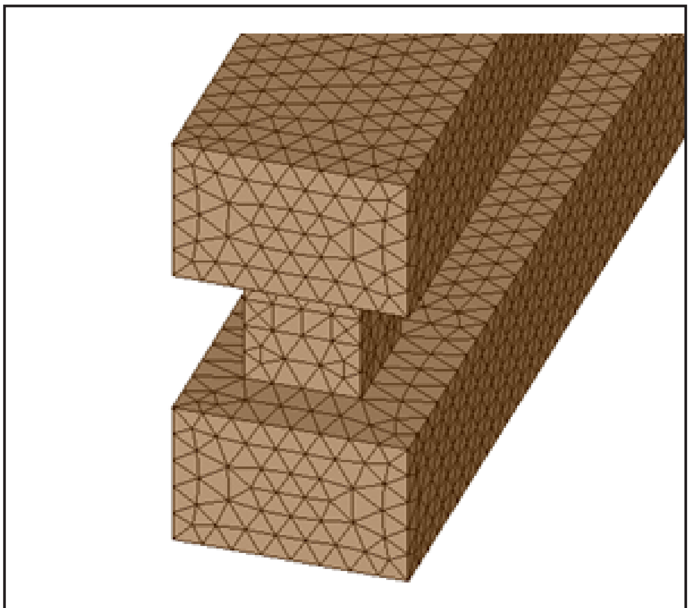

Fig. 2. Fragment of the FEM numerical model in the weld formation area along with the fragment of the arms and the visible mesh of finite elements

The numeral model used in the FEM calculations was a 3D electro-flow static model (DC flow). The model was composed of tetrahedral elements (tetrahedrons) and contained between 100 and 200 thousand finite elements (depending on the length of the arm; in relation to the base model - 130 thousand) and between 25 and 40 thousand nodes (in relation to the base model - 27 thousand). In terms of geometry, the structure of the model was as presented in Figure 1. The mesh of finite elements in the area of the electrodes and the weld is presented in Figure 2.

The FEM numerical model was used to determine the values of welding current in relation to various geometries of the arms, power density space distributions and voltages drops in the model as well as the space distribution of power (divided into the power emitted in the weld and power losses in the arms). The aforesaid calculation results are subjected to detailed analysis in the remainder of the article.

Results of simplified analytical calculations

The resistance (determined using dependence (1)) of the welding circuit in the function of the length of the arms and the cross-section of the electrodes as a parameter were used to determine (assuming the constant value of supply voltage) the values of current flowing in the circuit, the drop of voltage along the arms supplying current and corresponding power losses in the arms as well as power supplied to the weld. The variability of welding current in relation to a conductivity of 55 MS/m in the function of the (total) length of the arms ltot and the cross-section of the arms as a parameter are presented in Figure 3.

The results obtained in the simplified analytical calculations indicated that in relation to the basic case and depending on the dimensions of the arms (supplying current), the maintaining of constant supply voltage triggered changes in the values of current restricted within the

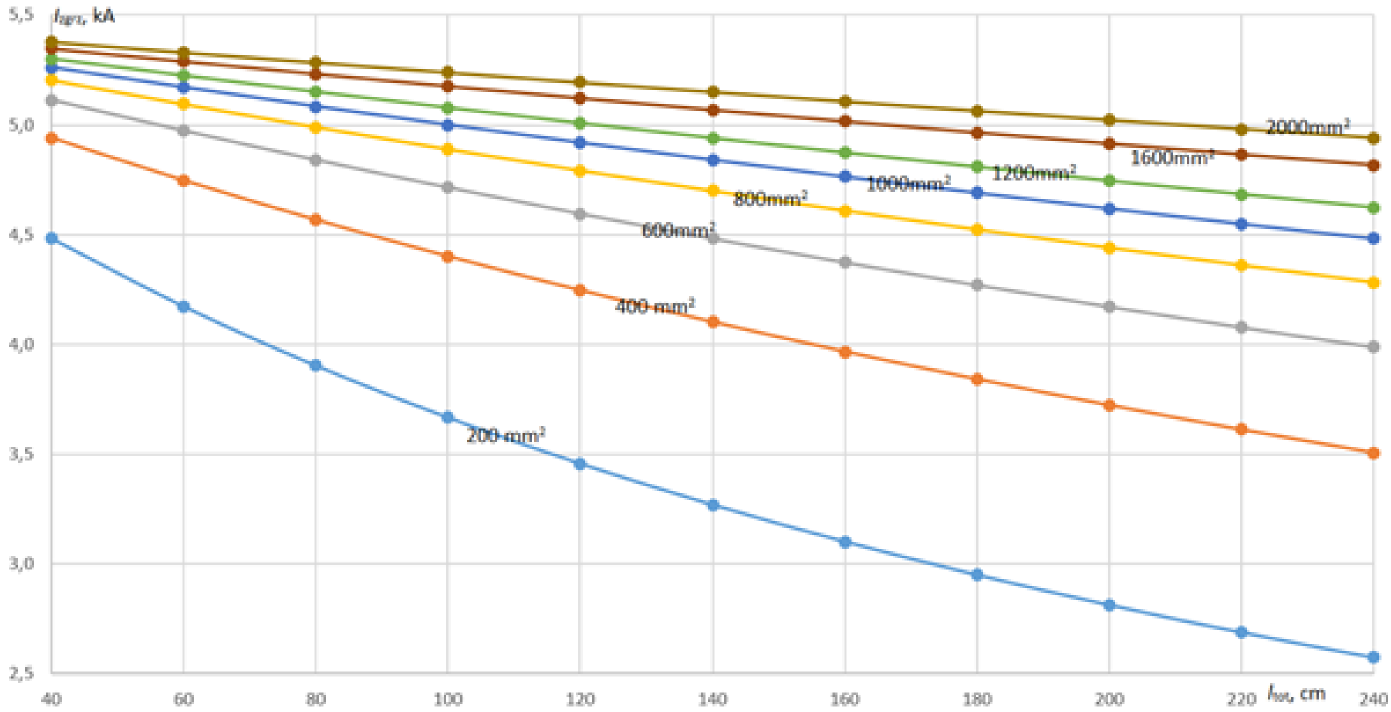

Fig. 3. Dependence of welding current on the length of the welding machine arms l_{tot} and their cross-section as a parameter in relation to constant supply voltage U_z = 2.2 V and on the assumption of constant operating temperature and a resultant copper conductivity of 55 MS/m

range of +7% (maximum current related to the largest cross-section and the shortest length of the arms) to -30% (in relation to the smallest cross-section and the longest length of the arms). In the extreme case (in relation to the longest arms having a cross-section of 200 mm2 the reduction of welding current could even amount to 50%). The aforesaid significant change could lead both to expulsion (in relation to a significant increase in current value) and the reduction of the diameter of the weld nugget or even its elimination (lack of the weld). The analysis of the data presented in Figure 3 demonstrated that the increase in length was accompanied by the decrease in current (minimum current value amounted to a little more than 2.5 kA if compared with a nominal current of 5 kA, i.e. nearly half as much). At the same time, the diagram revealed that in relation to any length it was possible to obtain the nominal current by using the appropriate cross-section of the arms (in relation to the arm having a cross-section of 2000 mm^2 and a total length of 240 cm, welding current was lower by nominal current by less than 100 A).

A tendency similar to that concerning the changes of welding current could be observed in relation to power supplied to the weld. However, it should be noted that in relation to the previously assumed averaged resistance of the weld, supplied power depended on squared current. The changes in values of power related to the length and the cross-section were even more visible (more significant) than those related to welding current.

Comparison of results obtained in FEM modelling with simplified results

The verification of the calculations performed using the simplified analytical method and the determination of inaccuracies resulting from the application of the method required the performance of the FEM-based comparative analysis of selected computational points. In relation to the basic case, the analysis revealed that that the resistance of the circuit determined in the FEM model was slightly higher than that determined in the simplified model (resistivity of the welding area was adjusted so that the resistance of the welding area was the same in both models). The foregoing could result from an increase in resistivity in the areas where the arms were bent as well as from an increase in resistivity in the area of the electrode. As a result, to obtain expected welding current it was necessary to use slightly higher supply voltage. The differences between the simplified model and the FEM model (in relation to the basic welding machine design) are presented in Table 1.

Table 1. Comparison of the primary parameters of the simplified analytical model and of the 3D FEM model

Parameter	Simplified model	FEM model
Static slope resistance	440 μΩ	503.7 μΩ
Weld resistance	400 μΩ	403.3 μΩ
Welding current in relation to voltage U_z=2.2 V	5.00 kA	4.36 kA
Voltage in relation to welding current I_{zg}=5 kA	2,200 V	2,519 V

The reason for the divergence between the simplified model and the 3D FEM model was confirmed by the analysis of current density in the structure subjected to analysis. Figure 4 presents the distribution of current density in the welding area. It is possible to notice the areas of changes in the direction of current overlapping with those related to changes in current density. The above-presented phenomenon could be observed in each bend of the electrode arm and was the reason for the divergence between the simplified model and the 3D FEM model. Current density was treated as uniform in the entire simplified model. The same method was used when analysing voltage drops (distribution of electric potentials) in the model. The analysis revealed that the distribution of voltage along the arms was uniform and, as such, did not significantly affect the differences between the simplified calculations and the FEM model-based calculations.

The performance of analysis involving various geometries of welding machine arms indicated that the tendencies of changes were maintained, which, in turn, indicated, that the simplified method-based analysis enabled the drawing of proper design-related conclusions within the comparative analysis of the system. Table 2 presents calculation results concerning selected parameters in relation to several various geometries based on the FEM model.

The obtainment of proper welding current in relation to given design parameters of the arms is possible by correcting voltage at the output of the power supply system (usually a

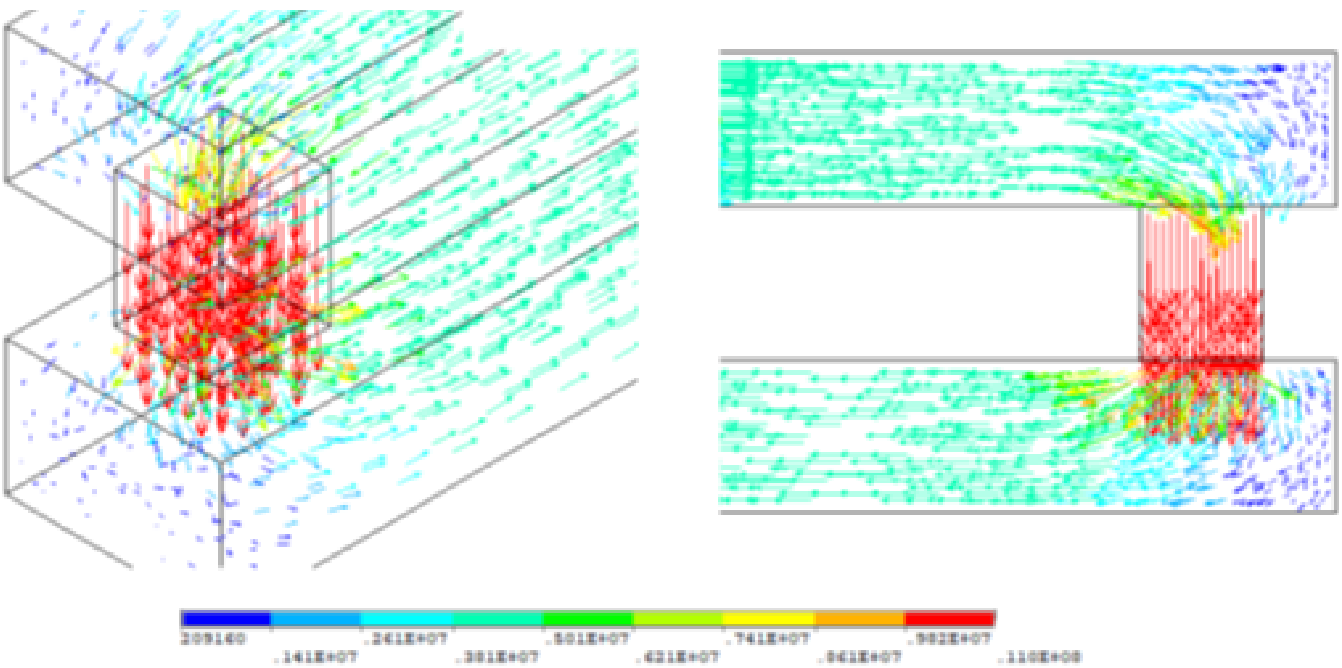

Fig. 4. Distribution of power density in the weld area determined on the basis of the 3D FEM numerical analysis

Table 2. Comparison of the primary parameters of the simplified analytical model and of the 3D FEM model

γ	l_p	s_1	Simplified model	FEM model	Difference %	Simplified model	FEM model	Difference %
			I_{zg}			P_{zg}		
MS/m	cm	mm²	kA		%	kW		%
55	60	600	4.71	4.68	-0.64	8.9	8.8	-1.14
	100		4.48	4.48	0.00	8.0	8.1	1.23
	140		4.27	4.28	0.23	7.3	7.4	1.35
	60	800	4.89	4.88	-0.20	9.6	9.6	0.00
	100		4.70	4.72	0.42	8.8	9.0	2.22
	140		4.52	4.56	0.88	8.2	8.4	2.38
	60	1000	5.00	5.00	0.00	10.0	10.0	0.00
	100		4.84	4.84	0.00	9.3	9.5	2.11
	140		4.69	4.72	0.64	8.8	9.0	2.22
	60	1200	5.08	5.08	0.00	10.3	10.4	0.96
	100		4.94	4.96	0.40	9.8	9.9	1.01
	140		4.81	4.84	0.62	9.3	9.5	2.11

transformer with a rectifying system). However, the issue gets complicated where a given power supply system powers (at the switch of an appropriate, usually electronic, switch) variously designed arms (having various lengths). The aforesaid situation takes place in terms of multispot systems where welding spots are located at various distances from the welding power source but should be powered by current of the same value.

The above-named problem could be solved by correcting not supply voltage at the terminals of the welding machine arms but by correcting their static slope resistance. If welding spots are located at various distances from the welding power source, the length of the arms could not be affected as this dimension is imposed by the location of a given welding spot. However, the resistance of the arms in relation to a given location can be corrected by changing the cross-section of the arm. The analysis indicated that it was possible to design the multispot welding machine arms so that an increase in a distance from the welding power source could be accompanied by an increase in the cross-section of the arm, thus maintaining the same static slope resistance of the circuit. When designing the welding circuit it is also necessary to pay attention to the density of transferred energy. For this reason, in a situation where more than one cross-section satisfies the requirements related to the minimum welding current it is necessary to adopt the solution characterised by the smallest possible cross-section and, at the same time, by the highest density of energy.

Another parameter directly affecting changes in the resistance of the arms and, consequently, changes in the values of current and power supplied to the welding area was a change in the arms operating temperature. The demonstration of the quantitative effect of a change in temperature on resistivity and, consequently, on current and power supplied to the weld required the performance of analysis, the results of which are presented in Figure 5. The above-presented data indicate that an increase in resistance was responsible for a decrease in power supplied to the weld by approximately 10% (also indicating an increase in power losses in the supply leads). At the same time, the above-presented data indicate that an increase in resistance led to a decrease in the range of cross-sections, in relation to which (for the specific length of the arms) it was possible to obtain the required value of welding current.

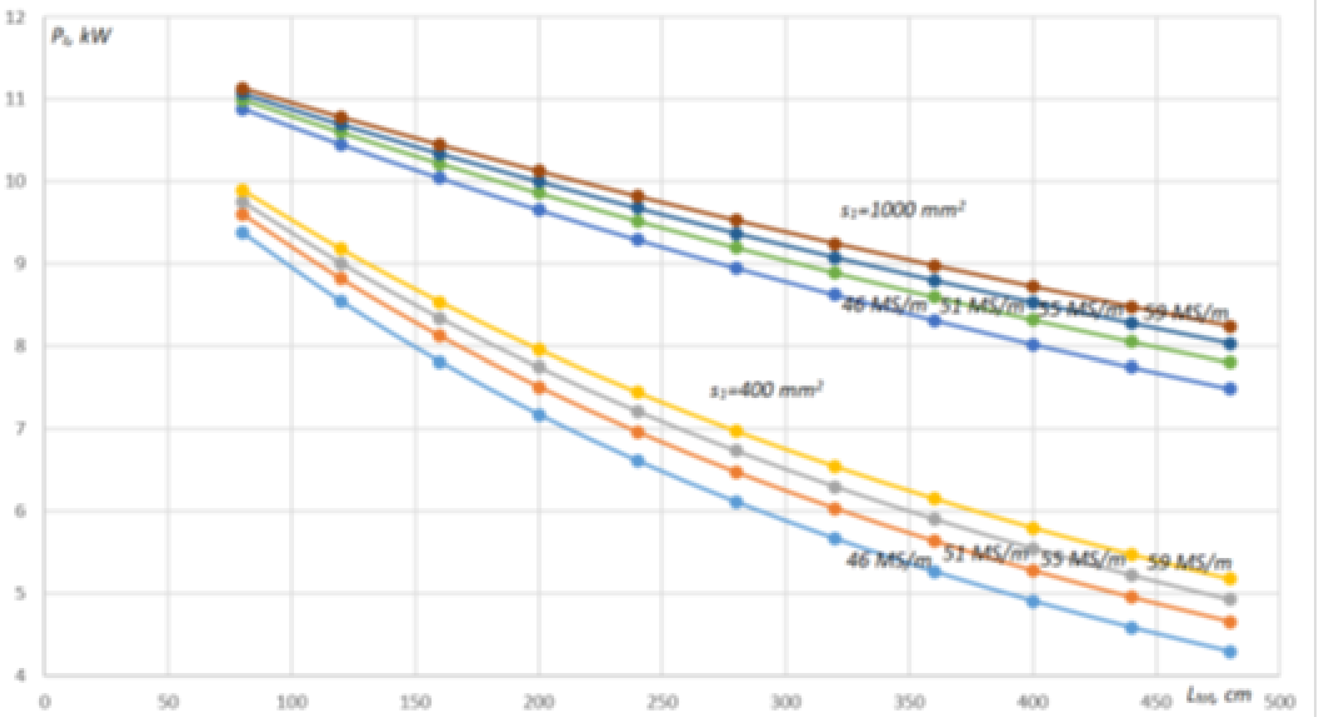

Fig. 5. Power supplied to the weld in the function of the length of the supply bars in relation to various values of resistivity and cross-sections of the bars as parameters

The analysis of power losses indicated the possibility of significant energy savings by changing the cross-section of the bars and their appropriate cooling. For instance, in relation to a total supply length of 200 cm the reduction of power losses was two-fold (from approximately 2 kW to approximately 1 kW). In relation to power supplied to the weld, the foregoing enabled saving approximately 10% of energy which, if combined with appropriate cooling could additionally decrease energy losses by 500 W. As a result, it could be possible to save up to approximately 15% of the total energy consumed by the welding machine output circuit. The reduction of power losses in the output circuit could also translate into the reduction of losses in the energy processing circuit of the welding machine (in the inverters and the transformer). As a result, it could be possible to reduce up to 20% of energy consumed by the welding machine in relation to the same process.

Analysis of welding current values on the weld diameter

The determination of the effect of welding current (dependent on the length and the cross-section of the welding machine arms) on the quality of welded joints required the development of an appropriate FEM numerical model and the performance of related calculations [4][5]. The analysis involved the numerical model of the cross-wise welding of bars presented in Figure 6. The calculations were performed in 3D. The parameters of the welding cycle included:

i) electrode force F=1.0 kN,

ii) welding time t_{zgrz} = 10 ms (current upslope time) + 20 ms (primary welding time)

iii) welding current within the range of I_{zg} = 3.0 kA to 5.0 kA [6] [7].

The numerical calculations involved the analysis of i) volume of the molten material of the weld nugget, ii) displacement of the electrodes (penetration of the bars) and iii) cross-sectional area of the weld nugget. Table 3 presents values obtained in the numerical calculations. Figure 7 presents the correlation between the area of the weld nugget and the value of welding current.

The calculations were performed in relation to bars (having a diameter of 4.0 mm and not provided with a protective coating) made of steel grade AISI10005. The calculations

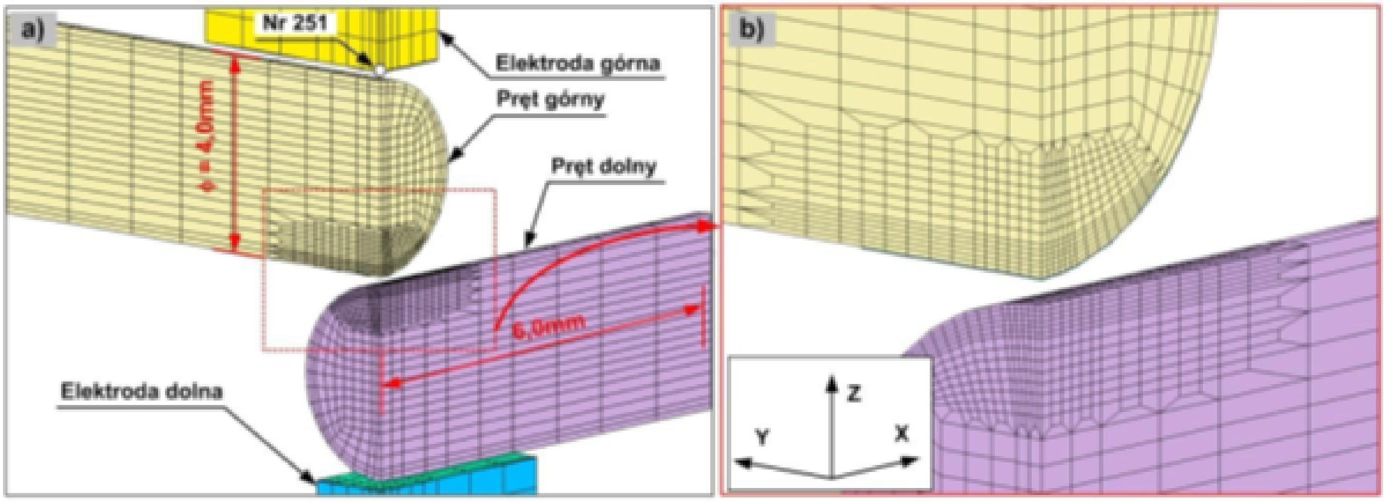

Fig. 6. Three-dimensional FEM model of the cross-wise welding of the bars

aimed to make it possible to observe the distribution of the temperature field in the welding area in relation to the primary parameter, i.e. the value of welding current. The characteristic parameters subjected to analysis included:

i) volume of molten metal,
ii) type of the weld nugget (full/ring-shaped),
iii) energy supplied to the weld,
iv) maximum temperature in the welding area,
v) penetration of the bars (displacement of the electrodes)
vi) weld nugget area.

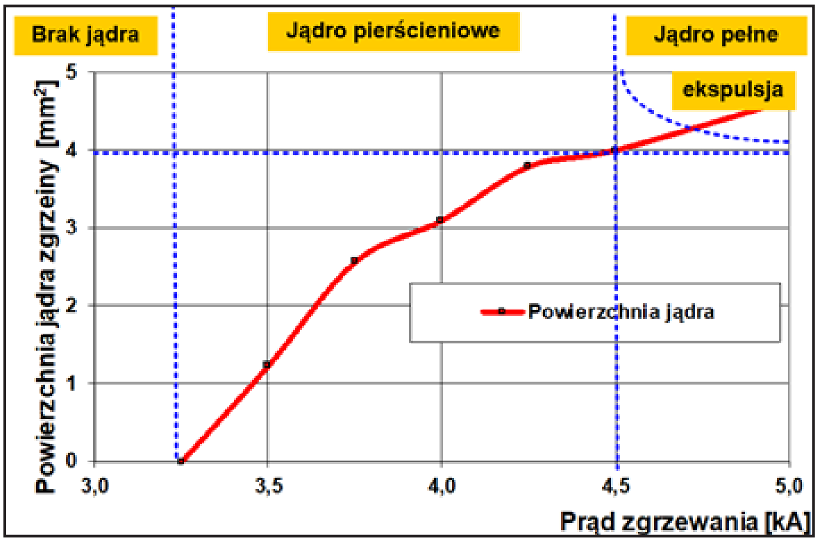

Fig. 7. Correlation between the weld nugget area and welding current

The crucial parameter in the above-presented analysis was the value of welding current I = 4.5 kA, in relation to which it was possible to obtain the full weld nugget. The above-named value enabled the appropriate adjustment of the length and the cross-section of the multispot welding machine arms, thus making it possible to obtain welds characterised by appropriate quality [8].

Table 3: Characteristic parameters of the cross-wise welding of bars

no.	Current	Volume of molten metal	Type of the weld nugget	Energy supplied to the weld	Max. temperature	Penetration of the bars Δl_{pp} max	Weld nugget area
	kA	mm³	-	J	°C	mm	mm²
1	3.00	0.12	lack	78	1520	-0.02	0
2	3.50	0.17	ring-shaped	84	1521	-0.22	1.23
3	3.75	0.35	ring-shaped	91	1536	-0.22	2.57
4	4.00	0.50	ring-shaped	97	1555	-0.24	3.10
5	4.25	1.19	ring-shaped	108	1575	-0.23	3.79
6	4.50	1.24	full	118	1590	-0.25	4.00
7	5.00	2.54	full	139	1631	-0.27	4.65

Summary and concluding remarks

The above-presented analysis justified the formulation of the following conclusions:

1. The tested changes in the resistance of the arms supplying current to the welding spot and the resultant decrease in welding current (where constant supply voltage was maintained) revealed that both the values of current and those of power supplied to the welding area decreased significantly within the ranges of changes in the design dimensions subjected to analysis.
2. The design of multispot welding machine arms characterised by various lengths and constant cross-section and powered by the same welding power source will result in the formation of welds characterised by various quality. In some situations welding could even prove impossible due to expulsion or because of the impossible formation of the weld nugget).
3. The proper external resistance of the arms could be achieved by appropriately changing their cross-sections in relation to length. The analysis revealed that in relation to each length of the arms it was possible to adjust a cross-section (also from the previously adopted range) preventing the loss of a welding current of more than 2%.
4. The results of the numerical calculations related to the welding of the bars revealed the formation of the full weld nugget above a current of 4.5 kA, where the remaining parameters included time of welding current flow (CPP, tPP) tzgrz = 30 ms (current upslope time amounted to 10 ms and the primary time of welding amounted to 20 ms) and electrode force F = 1.0 kN. The above-presented parameters appeared the most favourable. The correlation between the weld nugget area and the value of welding current revealed that a current decrease of 10% (from 4.5 kA to 4.0 kA) led to the reduction of the weld nugget area by 25% and, consequently, the reduction of the strength of the joint (weld). It should also be noted that the aforesaid unfavourably reduced parameters triggered the formation of the undesired ring weld nugget.
5. The analysis also indicated the important effect of changes in welding current and power losses resulting from changes in the temperature of the arms and, consequently, changes in the resistivity of the material conducting current. It is therefore justifiable to provide the appropriate cooling of the arms enabling the maintaining of appropriate operating temperature.

References:

[1] Wemet: Zgrzewarki wielopunktowe, http://www.wemet.eu/pl/produkty/zgrzewarki_wielopunktowe.html (accessed on 10.08.2020).

[2] Smoltech. Technika zgrzewalnicza. Inwertorowa zgrzewarka wielopunktowa. https://smoltech.pl/zgrzewarki-specjalizowane/inwertorowa-zgrzewarka-typu-sw-51-4x180/ (accessed on 10.08.2020).

[3] WiR Automation. Zgrzewarki wielopunktowe. https://wirautomation.pl/urzadzenia/zgrzewarki-wielopunktowe (accessed on 10.08.2020)

[4] SWANTEC – The database of the material and electrode parameters: model 2D .version 11.2 and model 3D Version 4.0x64 of the Swantec Inc. SORPAS Software.

[5] User Manual SORPAS® 2D Version 12, 2015, SWANTEC Software and Engineering ApS.

[6] Papkala H.: Resistance welding of metals. Publishing House KaBe Krosno, 2003.

[7] Pilarczyk J. (red.): Poradnik Inżyniera. Spawalnictwo, vol. 1. Wydawnictwa Naukowo-Techniczne, Warszawa, 1983.

[8] Dokumentacja Techniczno-Ruchowa zgrzewarek rezystancyjnych (ASPA, Smoltech), 2010.